Title

System-Dynamics Approach to Multireservoir Energy Generation under Climate Change

Journal

Journal of Hydrologic Engineering, 27(9)

ISSN

1084-0699

Authors

Rahmati, Kobra

Ashofteh, Parisa-Sadat

Afzali, Raheleh

et al.

Publication Date

2022-09-01

DOI

10.1061/(asce)he.1943-5584.0002197

Peer reviewed

ASCE

System-Dynamics Approach to Multireservoir Energy Generation under Climate Change

Kobra Rahmati[1]; Parisa-Sadat Ashofteh[2]; Raheleh Afzali[3]; and Hugo A. Loáiciga, F.ASCE[4]

Abstract: This paper evaluates several efficiency indexes of hydropower energy generation in Iran's Karkheh Basin water reservoir system (i.e., Seymareh and Karkheh Rivers) under climate change based on the system dynamics approach. The climate change effects are investigated with simulations of surface temperature and rainfall driven by downscaled climate projections from atmosphere–ocean circulation models in the current literature, and the models with the highest correlation and lowest error for rainfall and temperature in the 1976–2005 baseline period are identified. Rainfall and temperature are projected over two future periods, 2040–2069 and 2070–2099, and are downscaled to basin scale. Results project that the basin temperature over future periods will be higher than in the baseline period. Downscaled results under climate change indicate that rainfall will not follow a specific pattern. An artificial neural network applied to predict runoff indicates that the runoff and flood peak will decrease. Software is implemented to simulate the operation of hydropower reservoirs in baseline and future periods. Five reservoir operation states are considered, with simulation results of energy production showing that runoff and energy production have a complex pattern. Seven indexes of hydropower reservoir efficiency are also calculated for the five operation states corresponding to targets of energy production. **DOI: 10.1061/(ASCE)HE.1943-5584.0002197.**

Author keywords: Climate change; VENSIM; Efficiency indexes; System dynamics; Multireservoir hydropower system.

Introduction

Population , the resultant need for more energy, the reduction of nonrenewable energy sources, and environmental concerns call for the use of clean and renewable resources (Chen et al. 2016; Majumder et al. 2020). Hydropower is a source of renewable energy obtained from running water and its potential is affected by the hydrologic regime (Chilkoti et al. 2017). Hydropower and climate change phenomenon have a two-way relationship (Boadi and Owusu 2019); hydropower reduces climate change (Shrestha et al. 2021), and climate change affects hydropower generation by changing the temporal and spatial distribution of rainfall and consequent river discharge. This phenomenon reduces energy production in some hydropower plants (Adynkiewicz-Piragas and Miszuk 2020; Wang et al. 2019), and in some other cases is associated with increased energy fluctuations (Liu et al. 2020). Thus, climate change has emerged as a key issue for the management and development of hydropower plants in the future (Li et al. 2020). Given this two-way relationship between hydropower and climate change, it is important to understand how climate change is affecting water resources (Dallison et al. 2021). Studying the effects of climate change on hydropower projects can lead to timely response and adaptation (Jamali et al. 2013). Numerous studies have examined the effects of climate change on hydropower. For example, Mutsindikwa et al. (2021) investigated the effect of climate change in the Bamboi catchment. The results showed a reduction in discharge in the dry months, and an increase in discharge in the rainy season that could not be converted to hydropower. Zhong et al. (2020) used the Second-Generation Canadian Earth System Model (CanESM2) under the representative concentration pathway (RCP) 8.5 scenario to investigate the impact of climate change on hydropower energy in the Yangtze River Basin, which has an increasing trend.

Assessing climate change and its effects on hydropower generation is complex (Sarzaeim et al. 2018). In spite of such complexity predicting hydropower generation in the future is of utmost importance. Management decisions on energy generation must be based on the long-term status of water resources. Such decisions are aided by quantifying the effects of climate change on the system through performance indexes. Many studies have examined the impact of climate change on the basis of performance indexes of vulnerability, resiliency, flexibility, and sustainability (Alimohammadi et al. 2020; Nautiyal and Goel 2020; Zhou et al. 2020; Zeng et al. 2020; Ren et al. 2020). For example, Kim et al. (2019) evaluated the stability of the Boryeong multipurpose dam in terms of reliability, vulnerability, and flexibility based on climate change scenarios. Their results showed that flexibility and reliability would be reduced and the system would be vulnerable to drought scenarios. Zolghadr-Asli et al. (2019) applied the criteria of reliability, resiliency, and vulnerability to evaluate the impact of climate change uncertainty on the Karkheh Basin hydropower system. The results showed that the reliability and resiliency of the system improves under climate change and the vulnerability of the system would be increased due to the occurrence of water shortage. This showed that, although the system would not experience frequent crashes, severe blackouts may occur. Fan et al. (2020) examined the impact of climate change on hydropower generation based on RCP scenarios in different parts of China. The results showed that hydropower plants were vulnerable and sensitive to climate fluctuations.

[1]Master's Student, Dept. of Civil Engineering, Univ. of Qom, Qom 3716146611, Iran. Email: K.Rahmati@stu.qom.ac.ir

[2]Associate Professor, Dept. of Civil Engineering, Univ. of Qom, Qom 3716146611, Iran (corresponding author). Email: PS.Ashofteh@qom.ac.ir

[3]Water Resources Engineer, Mahab Ghodss Consulting Engineering Company, Dastgerdy, Tehran 1918783414, Iran. Email: raheleh.afzali@gmail.com

[4]Professor, Dept. of Geography, Univ. of California, Santa Barbara, CA 93016-4060. Email: hloaiciga@ucsb.edu

Note. This manuscript was submitted on July 7, 2021; approved on May 2, 2022; published online on June 25, 2022. Discussion period open until November 25, 2022; separate discussions must be submitted for individual papers. This paper is part of the ***Journal of Hydrologic Engineering***, © ASCE, ISSN 1084-0699.

Nguyen et al. (2020) used the criteria of reliability, vulnerability, and resiliency to assess the effects of climate change on reservoir storage in Australia. Their results showed that reliability and flexibility would decline and vulnerability would rise. Qin et al. (2020) evaluated the effects of climate change on the performance of the Gorges three-reservoir system by five general circulation models (GCMs) under RCP scenarios. Their results showed that the response of power generation to climate change would follow a nonlinear pattern in which increasing river flow does not lead to increasing hydropower generation. Obahoundje et al. (2021) evaluated climate change, land use, and development conditions on hydropower generation using regional climate models (RCMs) in the Mono basin, Togo. The later authors applied water evaluation and planning (WEAP) for simulating the water availability. The results of climate simulation showed that the temperature does not increase significantly and rainfall does not show a specific trend. Also, climate change affects water use and especially energy production.

The Sazban, Seymareh, and Karkheh hydropower reservoirs in the Karkheh basin, Iran, serve as the case study for this paper's methodology. This study evaluated five operation states of the hydropower reservoir system. The first and second operation states consisted of the independent operation of the Sazbon and Seymareh reservoirs, respectively. The third and fourth states were the operation of a two-reservoir system; Seymareh and Sazbon reservoirs made up the third operation state, and Karkheh and Seymareh reservoirs were the fourth operation state. The fifth state consisted of the operation of a three-reservoir system (Sazbon, Seymareh, and Karkheh reservoirs) under climate change based on seven reservoir efficiency indexes (time reliability, volume reliability, vulnerability, resiliency, sustainability, availability, supply to demand). Hydropower produced by the five operation states is simulated with VENSIM software for the baseline (1976–2005) and climate change (2040–2069 and 2070–2099) periods. The Fifth Assessment Report (AR5) of the Intergovernmental Panel on Climate Change (IPCC) provides the climate projections for this work. The hydropower energy is simulated in the baseline and future periods and is evaluated with seven reservoir efficiency indexes mentioned previously.

Methods and Materials

The present study consists of six parts. The first part examines the climate projections of 17 atmospheric/ocean GCMs (AOGCMs) and selects the best performing model or models. The second part generates climate scenarios of temperature and rainfall at basin scale. The third part projects future runoff using an artificial neural network (ANN). The fourth section introduces the governing equations in hydropower reservoir system. The fifth section presents simulation results of operation of hydropower reservoirs calculated with VENSIM software. The sixth section evaluates the effects of climate change on operation of hydropower reservoirs based on reservoir efficiency indexes. A schematic of this paper's methodology is displayed in Fig. 1.

Evaluation of Climate Models

The climate projections of the AOGCMs in baseline (1976–2005) are compared with the corresponding observed values to measure the models' performance. The IPCC introduced the RCPs to produce a series of climate projections in its Fifth Assessment Report. The new scenarios are based on their radiation forcing (RF) levels by the end of the 21st century, with RF equal to 8.5, 4.5, and 2.6 $W/(m^2\ s)$ corresponding to RCP8.5, RCP4.5, and RCP2.6, respectively (IPCC 2013). This study evaluated 17 GCMs applied in the IPCC's AR5. The GCMs evaluation led to selection of the best-performing GCMs for investigating the effect of climate change on hydropower generation. The evaluation of AOGCMs' climate projections was based on several goodness-of-fit criteria. These are the correlation coefficient (r), root mean-square error (RMSE), mean absolute error (MAE), and Nash-Sutcliffe efficiency (NSE) (Nash and Sutcliffe 1970) [see Moriasi et al. (2007), for a discussion of these criteria]. The formulas for the criteria are given as follows:

$$r = \frac{\sum_{i=1}^{N}(X_s - \bar{X}_s)(X_m - \bar{X}_m)}{\sqrt{\sum_{i=1}^{N}(X_s - \bar{X}_s)^2 \sum_{i=1}^{N}(X_m - \bar{X}_m)^2}} \tag{1}$$

$$\text{RMSE} = \sqrt{\frac{\sum_{i=1}^{N}(X_s - X_m)^2}{N}} \tag{2}$$

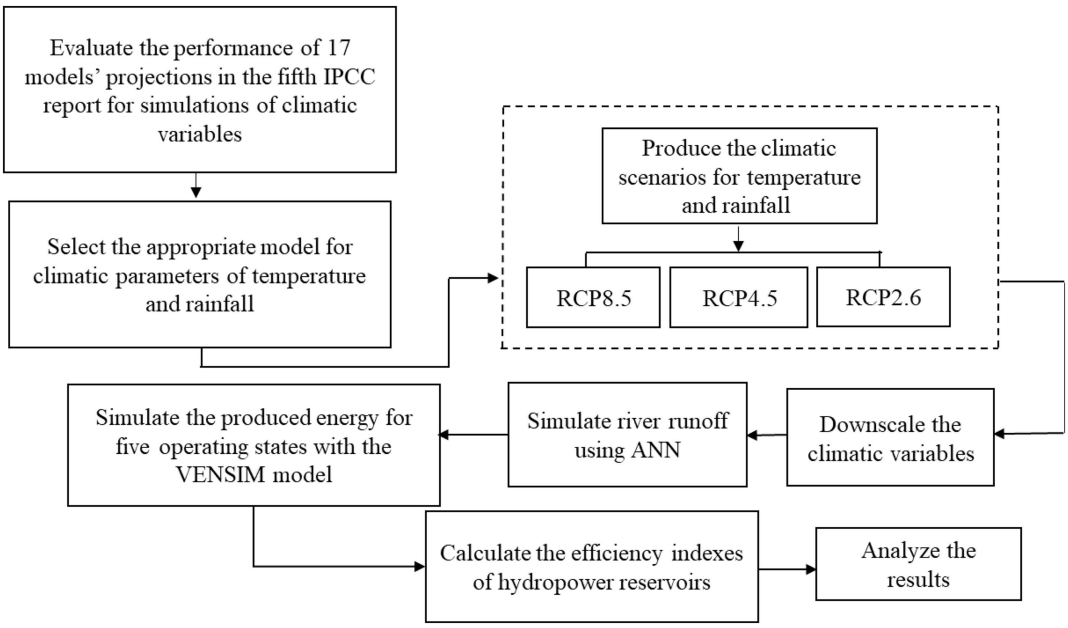

Fig. 1. Workflow of study methodology.

J. Hydrol. Eng., 2022, 27(9): 04022018

$$\mathrm{MAE} = \frac{\sum_{i=1}^{N} |X_s - X_m|}{N} \tag{3}$$

$$\mathrm{NSE} = 1 - \frac{\sum_{i=1}^{N} (X_m - X_s)^2}{\sum_{i=1}^{N} (X_m - \bar{X}_m)^2} \tag{4}$$

where X_s = model simulation data; X_m = observed data; $\bar{X}_s$ = average data from model simulation; and $\bar{X}_m$ = average observed data.

The evaluation of the performance of the GCMs leads to the selection of the best AOGCMs, and this is followed by generation of the climate scenarios with downscaled variables applied to basin-scale runoff projections.

Generation of Climate Scenarios and Downscaling of Climatic Variables

Climate scenarios of temperature and rainfall in study area were calculated from IPCC's AOGCM projections according to Eqs. (5) and (6) (Jones and Hulme 1996)

$$\Delta TEM_t = (\overline{TEM}_{GCM,FUT,t} - \overline{TEM}_{GCM,BAS,t}) \tag{5}$$

$$\Delta RAI_t = \left(\frac{\overline{RAI}_{GCM,FUT,t}}{\overline{RAI}_{GCM,BAS,t}}\right) \tag{6}$$

where ΔTEM_t = climate change projection of surface air temperature; $\overline{TEM}_{GCM,FUT,t}$ = average long-term surface air temperature simulated by the GCMs in a future period of climate change; $\overline{TEM}_{GCM,BAS,t}$ = average long-term surface air temperature simulated by the GCMs in baseline; ΔRAI_t = climate change projection of rainfall; $\overline{RAI}_{GCM,FUT,t}$ = average long-term rainfall simulated by GCMs in a period of climate change; and $\overline{RAI}_{GCM,BAS,t}$ = average long-term rainfall simulated by GCMs in the baseline period.

One approach to overcome the coarse resolution of AOGCMs is the downscaling of their outputs. This work implements the proportional method for downscaling [Eqs. (7) and (8)]

$$TEM_{FUT} = TEM_{OBS} + \Delta TEM \tag{7}$$

$$RAI_{FUT} = RAI_{OBS} \times \Delta RAI \tag{8}$$

where TEM_{OBS} = monthly time series of observed temperature; TEM_{FUT} = monthly time series of future temperature; RAI_{OBS} = monthly time series of observed rainfall; and RAI_{FUT} = monthly time series of future rainfall.

The simulated monthly time series of temperature and rainfall in future periods are input to simulate river discharge.

Simulation of River Discharge

This work applies ANNs to predict the flow of the Seymareh and Karkheh Rivers in two future periods. The performance of ANN in this paper is evaluated with the statistical criteria r [Eq. (1)], percent bias (PB) (Gupta et al. 1999; Moriasi et al. 2007), NSE [Eq. (4)], and RMSE over observations' standard deviation ratio (RSR) (Moriasi et al. 2007). The PB and RSR are calculated based on Eqs. (9) and (10), respectively

$$\mathrm{PB} = \left[\frac{\sum_{t=1}^{N}(X_t^{obs} - X_t^{sim})}{\sum_{t=1}^{N} X_t^{obs}}\right] \times 100\% \tag{9}$$

$$\mathrm{RSR} = \left[\frac{\sqrt{\sum_{t=1}^{N} (X_t^{obs} - X_t^{sim})^2}}{\sqrt{\sum_{t=1}^{N} (X_t^{obs} - X_{\mathrm{mean}}^{obs})^2}}\right] \tag{10}$$

where X_t^{obs} = observed variable in time step t; X_t^{sim} = simulated variable in time step t; and X_{mean}^{obs} = average observed variable.

A value of NSE larger than 0.5, RSR less than 0.7, and PB between −25% and 25% are evidence of accurate simulation results (Moriasi et al. 2007).

Equations Governing Hydropower Generation by a System of Reservoirs

Reservoir volume balance is described by Eq. (11)

$$S_{i,t+1} = S_{i,t} + Q_{i,t} - RE_{i,t} - LOSS_{i,t} - SP_{i,t} \tag{11}$$

where $S_{i,t+1}$ = storage in reservoir i at the beginning of the period $t+1$ ($\times 10^6$ m^3); $S_{i,t}$ = storage in reservoir i at the beginning of the period t ($\times 10^6$ m^3); $Q_{i,t}$ = inflow volume to reservoir i during the period t ($\times 10^6$ m^3); $RE_{i,t}$ = release volume from the reservoir i during the period t ($\times 10^6$ m^3); $LOSS_{i,t}$ = loss of storage in reservoir i during period t ($\times 10^6$ m^3); and $SP_{i,t}$ = spill volume from reservoir i during period t ($\times 10^6$ m^3).

The reservoir spill constraint ($SP_{i,t}$) in Eq. (11) depends on reservoir storage in period t. Let $V_{i,t+1} = S_{i,t} + Q_{i,t} - RE_{i,t} - LOSS_{i,t}$; reservoir spill constraint is written as follows:

$$SP_{i,t} = \begin{cases} V_{i,t+1} - S_{\max,i} & \text{if } V_{i,t+1} > S_{\max,i} \\ 0 & \text{else} \end{cases} \tag{12}$$

where $S_{\max,i}$ = maximum storage volume of reservoir i ($\times 10^6$ m^3).

Power plant capacity, net loss in reservoir water, and power plant energy production are calculated according to Eqs. (13)–(15), respectively

$$P_{i,t} = \frac{RE_{i,t} \times g \times e_i \times H_{i,net}}{1{,}000} \tag{13}$$

$$H_{i,net} = ELV_i - TW_i - H_{f,i} \tag{14}$$

$$E_i = \frac{P_i \times \mathrm{PeakHour}_i \times \mathrm{day}}{1{,}000} \tag{15}$$

where g = gravity acceleration (m/s^2); e_i = efficiency of power plant i; $H_{i,\mathrm{net}}$ = net loss of water in reservoir i; $P_{i,t}$ = capacity of power plant i during period t (MW); ELV_i = reservoir water level i; TW_i = water level at the downstream of power plant i; $H_{f,i}$ = reservoir head drop i; day = number of days of the month; $\mathrm{PeakHour}_i$ = peak hour for power generation of each power plant i; and E_i = energy produced by power plant i (GWh).

Other constraints on problem include constraints on reservoir storage volume and release volume, which are given in Eqs. (16) and (17), respectively

$$RE_{\min,i} \le RE_{i,t} \le RE_{\max,i} \tag{16}$$

$$S_{\min,i} \le S_{i,t} \le S_{\max,i} \tag{17}$$

where $RE_{\min,i}$ = minimum release volume of reservoir i ($\times 10^6$ m^3); $RE_{\max,i}$ = maximum release volume of reservoir i ($\times 10^6$ m^3); and $S_{\min,i}$ = minimum storage volume of reservoir i ($\times 10^6$ m^3).

Simulation of Operation of Hydropower Reservoir with VENSIM Model

System dynamics is based on systems reasoning about event processes, and systematically deals with complexities of a system whose operation is optimized to achieve defined objectives. This work uses VENSIM software, which is based on system dynamics, to simulate the reservoir system. VENSIM is designed to model one or more quantities that change over time applying correct understanding of system components and their interactions. System

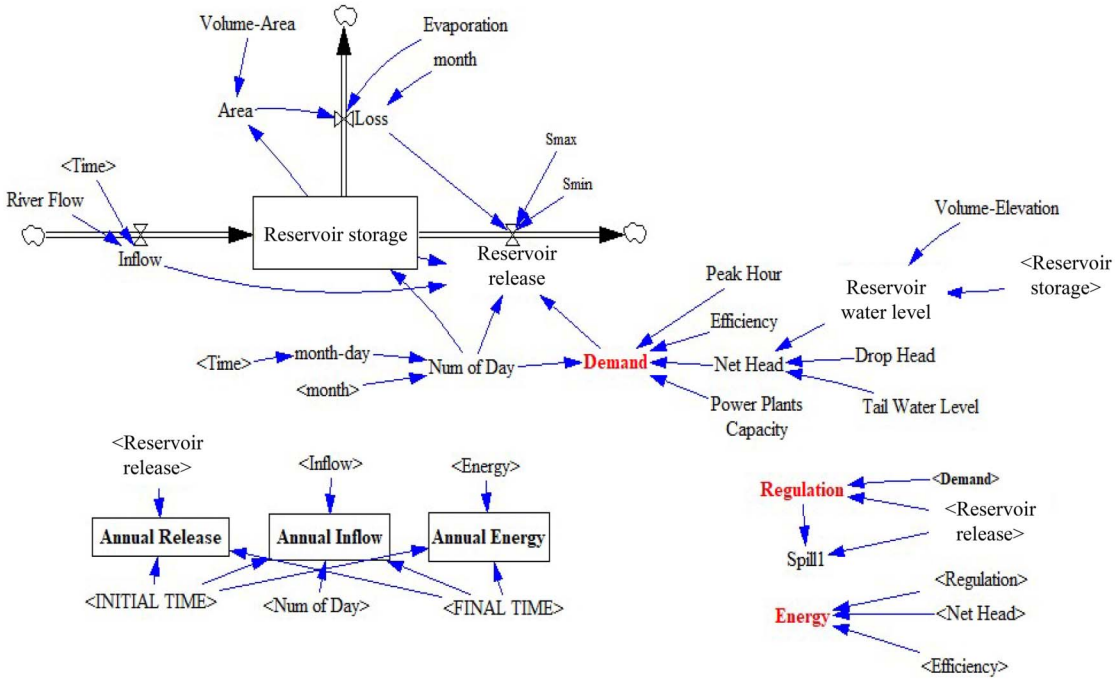

Fig. 2. Display of single-reservoir model in VENSIM.

components in VENSIM are defined as state, rate, and auxiliary variables. The state variable is the result of an accumulation of rate variables that have a certain value at the beginning of the simulation period. The flow variable changes the size of the state variable at each time step. The flow variable is key to determining the behavior of the state variable. An auxiliary variable, which is an equation or constant number, is used to relate system variables. VENSIM introduces and defines the relationships between variables by means of arrows. Arrows transmit inputs and information. Fig. 2 depicts the single-reservoir system model with VENSIM conventional signs.

Efficiency Indexes of Hydropower Reservoir

Hashimoto et al. (1982) defined indexes such as reliability, vulnerability, and resiliency to evaluate the performance of water resource systems. Time reliability is defined as the ratio of number of periods in which total energy produced as equal to or greater than α percent of power plant's energy production capacity (EPC) to total number of operational time periods, obtained from Eq. (18)

$$RT = \frac{1}{T}\sum_{t=1}^{T} n_t \tag{18}$$

where $n_t = 1$ if $(\sum_{i=1}^{N} E_{i,t} \geq \alpha \sum_{i=1}^{N} \mathrm{EPC}_i)$, else $n_t = 0$; $E_{i,t}$ = the energy produced by reservoir i in the time step t; RT = time reliability; EPC_i = energy production capacity of power plant i (GWh); T = total number of time periods; N = total number of reservoirs; α = percentage of energy production capacity; and $(\sum_{i=1}^{N} E_{i,t} \geq \alpha \sum_{i=1}^{N} \mathrm{EPC}_i)$ = the number of periods when the total energy is equal to or greater than the percentage of the power plant's energy production capacity.

Volumetric reliability is defined as the ratio of total energy produced to the energy production capacity of power plant during operation [Eq. (19)]

$$RV = \frac{1}{T}\sum_{t=1}^{T} \frac{\mathrm{Min}(\sum_{i=1}^{N} E_{i,t}, \alpha \sum_{i=1}^{N} \mathrm{EPC}_i)}{\alpha \sum_{i=}^{N} \mathrm{EPC}_i} \tag{19}$$

where RV = volumetric reliability.

Resiliency expresses the speed of failure recovery and is calculated from Eq. (20)

$$R = \frac{1}{T_f}\sum_{t=1}^{T-1} y_t$$
$$T_f = \sum_{t=1}^{T} Z_t \tag{20}$$

where R = speed of resiliency; $y_t = 1$ if $[(\sum_{i=1}^{N} E_{i,t} < \alpha \sum_{i=1}^{N} \mathrm{EPC}_i)$ and $(\sum_{i=1}^{N} E_{i,t+1} \geq \alpha \sum_{i=1}^{N} \mathrm{EPC}_i)]$ else $y_t = 0$; $[(\sum_{i=1}^{N} E_{i,t} < \alpha \sum_{i=1}^{N} \mathrm{EPC}_i)$ and $(\sum_{i=1}^{N} E_{i,t+1} \geq \alpha \sum_{i=1}^{N} \mathrm{EPC}_i)]$ = periods in which the system succeeds after failure; T_f = total number of failure periods; and $Z_t = 1$ if $(\sum_{i=1}^{N} E_{i,t} < \alpha \sum_{i=1}^{N} \mathrm{EPC}_i)$ else $T_f = 0$.

Vulnerability represents the sum of deficiencies that it is calculated according to Eq. (21)

$$V = \frac{1}{T}\sum_{t=1}^{T} \frac{\alpha \sum_{i=1}^{N} \mathrm{EPC}_i - \sum_{i=1}^{N} E_{i,t}}{\alpha \sum_{i=1}^{N} \mathrm{EPC}_i} \tag{21}$$

where V = vulnerability.

Reliability, resiliency, and vulnerability indexes are combined in a sustainability index that makes it possible to compare alternative projects and policies (Loucks 1997)

$$S = R \times RT(1 - V) \tag{22}$$

where S = sustainability.

Availability according to Eq. (23) is the capacity of the system to meet the demands downstream of a dam (Ashofteh et al. 2019)

$$\xi = prob(E_{i,t} \geq \alpha \mathrm{EPC}_{i,t} | \alpha \mathrm{EPC}_{i,t} \neq 0) \quad (23)$$

where ξ = availability; and $prob$ = probability that the energy produced is greater than or equal to the production capacity.

The supply-to-demand index as defined by ASCE (1998) is calculated with Eq. (24)

$$STD = \sum_{t=1}^{T} \frac{SUP_t}{\lambda}$$

$$SUP_t = \begin{cases} \alpha EGC_i & \text{if } E_{i,t} \geq \alpha EGC_i \\ \alpha EGC_i - E_{i,t} & \text{else } E_{i,t} < \alpha EGC_i \end{cases}$$

$$\lambda = \sum_{t=1}^{T} \alpha EGC_i \quad (24)$$

where SUP = energy production capacity (if the energy produced is greater than or equal to the production capacity); λ = energy production capacity at the time t; and STD = index of supply to demand.

Case Study

The Karkheh basin is located to the west and southwest of the Zagros Mountains in western Iran, and is a part of the Persian Gulf basin in terms of the general hydrological setting of Iran.

Table 1. Specifications of basin stations

Station name	Station type	Elevation (m)	Longitude	Latitude
Ghurbaghestan	Rain gauge	1,320	47.15	34.14
Pol-Chehr	Climatology	1,275	47.43	34.34
Nazar-Abad	Hydrometric	530	47.28	33.11
Cham-Gaz	Rain gauge	380	49.78	32.95
Abdolkhan	Climatology	40	48.38	31.83
Jelogir	Hydrometric	350	47.48	32.58

The Karkheh basin is limited to the north by the Sirvan, Sefidrood, and Qarachai Rivers, and to the west by the Border Rivers between Iran and Iraq, to the east by the Dez River, and to the south by a part of the western border of the country. The area of the Karkheh basin is 51,604 km^2. This work studies the Sazbon, Seymareh, and Karkheh hydropower production. The characteristics of the stations surveyed in the basin are listed in Table 1. A map of the Karkheh basin and its reservoirs is displayed in Fig. 3. The specifications of the studied reservoirs are listed in Table 2.

The temperature data of the Polchehr and Abdolkhan climatology stations were used for the Seymareh and Karkheh Rivers, respectively. Also, the data from the Qurbaghistan Cham-Gaz rainfall gauge station were applied to Seymareh and Karkheh Rivers, and the streamflow data from the Nazarabad and Jeloghir hydrometric stations (streamflow) were used for Seymareh and Karkheh Rivers, respectively, over a period of 30 years, i.e., 1976–2005. The observed long-term time series of temperature, rainfall, and runoff of both rivers are shown in Fig. 4. Also, the average long-term monthly observed values for temperature, rainfall, and runoff are given in Fig. 5. Fig. 5 shows that the maximum and minimum long-term average monthly temperature values in the Seymareh (Polchehr station) and Karkheh (Abdolkhan station) Rivers are taken in July and January, and are 26.16°C and 3.54°C (for the Seymareh River), and 35.66°C and 12.3°C (for the Karkheh river), respectively. The maximum and minimum of average long-term monthly rainfalls in the Seymareh (Qurbaghistan) and Karkheh (Cham-Gaz) Rivers happen in December and July, and are 56.16 and 0.39 mm (for the Seymareh River), and 90.18 and 0.1 mm (for the Karkheh River), respectively. The maximum and minimum average long-term monthly runoff for the Seymareh River (Nazarabad) happens in April and September with 193.66 and 26.81 m^3/s; for the Karkheh River (Jeloghir) this is in April and August with 316.91 and 37.51 m^3/s.

The climate of an area depends on several factors, including the circulation of air masses. Air masses that affect Karkheh Basin

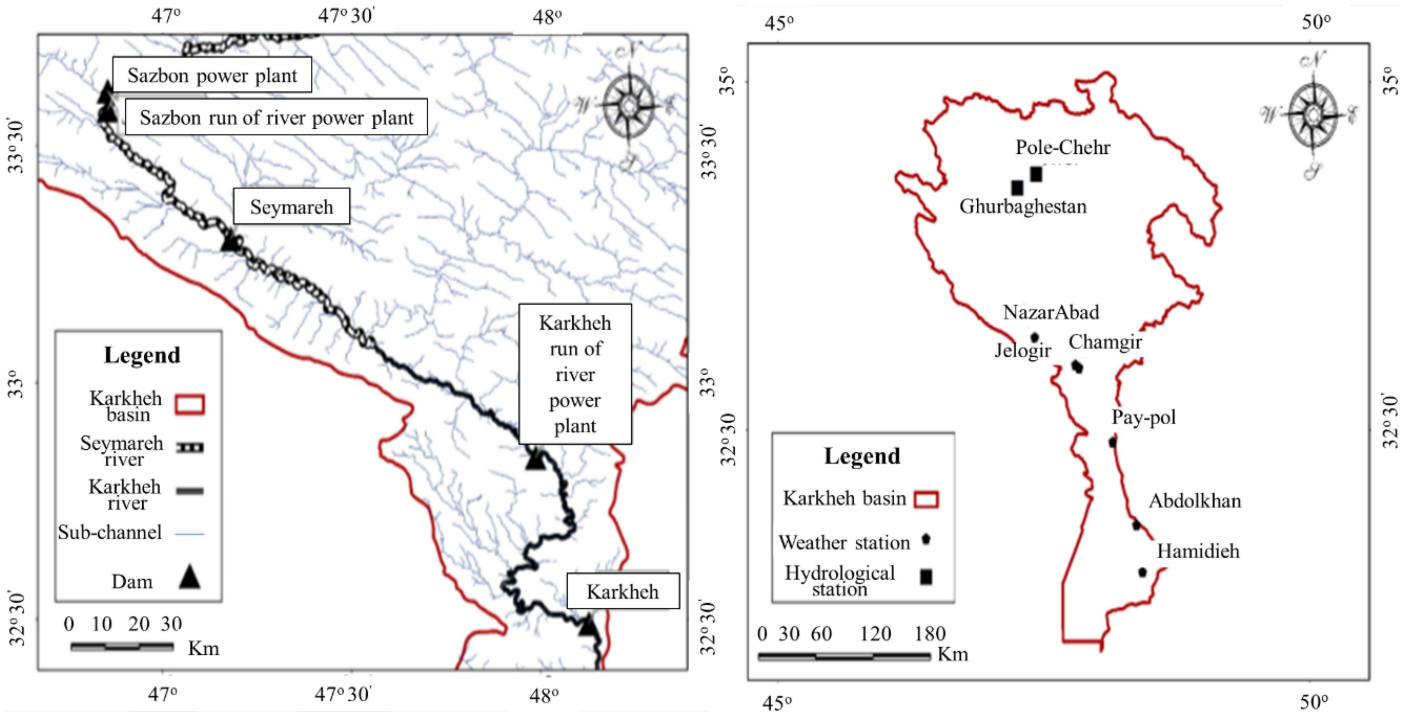

Fig. 3. Location of the basin and reservoirs in the study area.

Table 2. Specifications of reservoirs

Characteristics	Reservoir		
	Sazbon	Seymareh	Karkheh
Reservoir normal water level (m above sea level)	850	720	375
Reservoir minimum water level (m above sea level)	830	705	370
Reservoir volume at normal water level ($\times 10^6$ m^3)	1,575.7	2,473.6	131.7
Reservoir volume at minimum water level ($\times 10^6$ m^3)	918.2	1,663.6	92.38
Installed hydropower capacity (MW)	300	480	360
Performance coefficient of the power plant	0.16	0.16	0.25
Power plant efficiency	0.93	0.935	0.93
Purpose	Hydropower	Hydropower	Hydropower

include maritime tropical air (which mostly enters Iran during the cold seasons from the west and southwest), maritime polar air (which enters from the north and northwest of Iran), the continental polar air [which enters from the northeast (Siberia) and the northwest (northern Europe)], and continental tropical air mass (which sometimes enters Iran from Saudi Arabia and North Africa in the south and southwest). Thus, the climate of Karkheh Basin is governed by several regional sources of air circulation.

Results

Results of AOGCMs

The best AOGCMs climate projections were selected among those of 17 models reported in the fifth IPCC report. The projections were vetted with the *r*, RMSE, MAE, and NSE criteria. The results listed in Table 3 indicate most of the models simulate the basin temperature and rainfall well. The CNRM-CM5 (Centre National

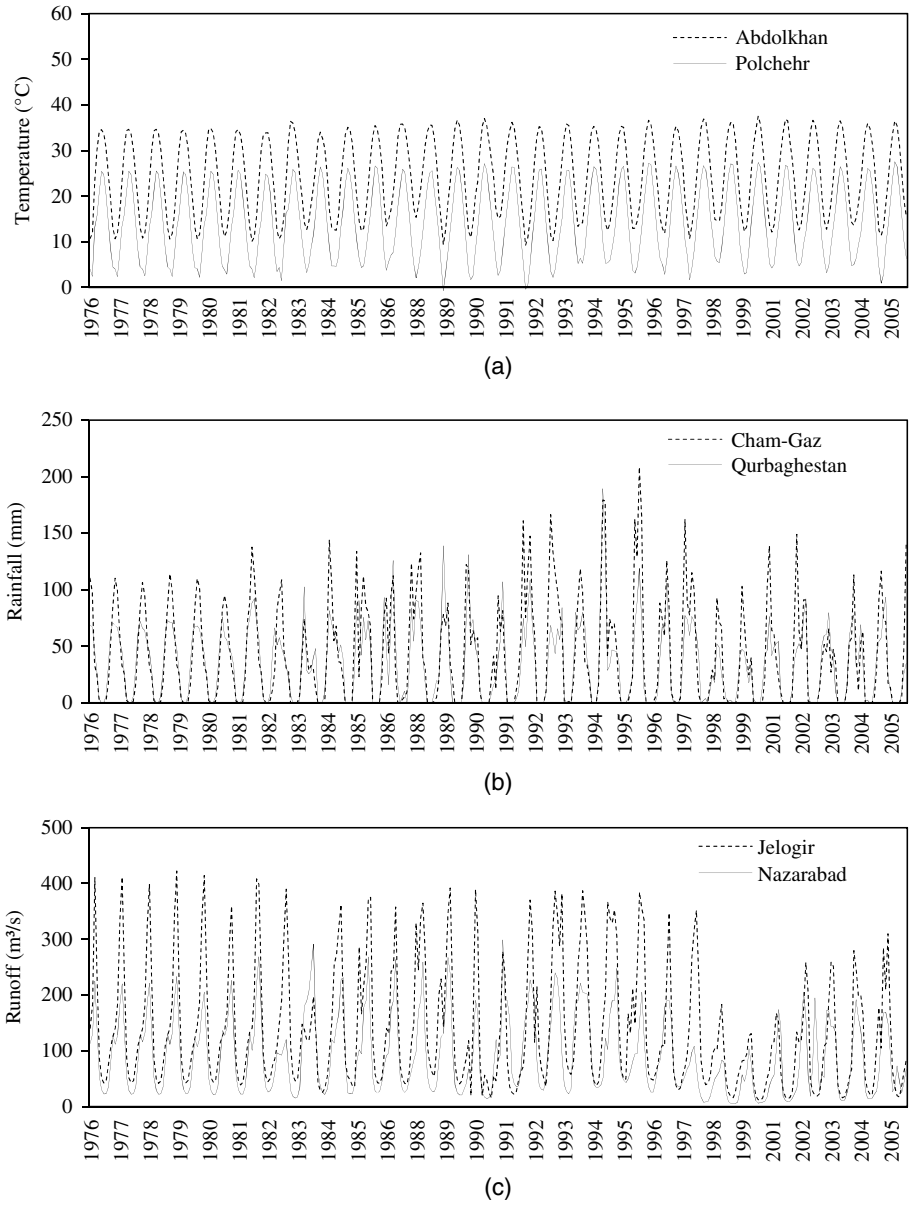

Fig. 4. Time series of observed values of (a) temperature; (b) rainfall; and (c) streamflow.

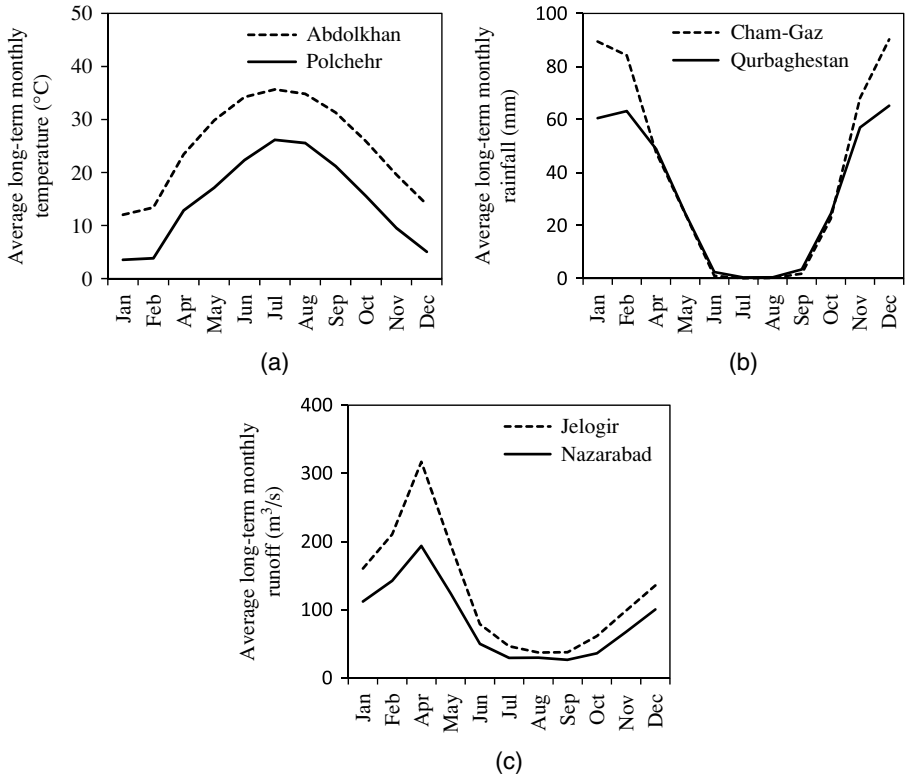

Fig. 5. Average long-term monthly observed values of (a) temperature; (b) rainfall; and (c) streamflow.

Table 3. Performance criteria of AOGCMs compared to the observation period

	Rainfall				Temperature			
Climate model	r (%)	RMSE (mm)	MAE (mm)	NSE (dimensionless)	r (%)	RMSE (mm)	MAE (mm)	NSE (dimensionless)
BCC-CSM1-1	81.8	39.7	28.2	−0.2	99.6	6.6	6.6	0.6
BCC-CSM1-1-M	93.5	36.2	27.2	−0.1	99.6	6	6	0.6
CESM1-CAM5	76.2	32.1	23	−0.3	99.7	6.2	7.2	0.5
MIROC-ESM	46.7	41	3	−0.3	99	3.3	3	0.9
MIROC ESM-CHEM	49.9	40.3	31	−0.2	98	3	2.8	0.9
MPI-ESM-LR	95	29	22	0.3	99.8	4.8	4.7	0.7
MPI-ESM-MR	89	27.5	19	−0.4	99.7	5.4	5.3	0.7
NorESM1-M	31.3	48.5	34.9	−0.8	99.3	2.7	2.4	0.9
CNRM-CM5	87	17.9	13.5	0.8	99.8	11.3	11.3	−0.2
GISS-E2-H	90	45.8	34	−0.6	99.3	5.7	5.3	0.7
GISS-E2-R	71.73	42.15	30.3	−0.37	99.6	5	4.8	0.8
GFDL-CM3	53	43.9	76.2	−0.5	99.6	2.1	2.1	0.9
GFDL-ESM2G	75.81	40.7	28.9	−0.3	99.3	2.9	2.7	0.9
GFDL-ESM2M	49.6	46.9	34	−0.7	99.3	2.1	1.8	0.9
CCSM4	79.8	27.31	21.5	0.5	99.6	2.7	2.6	0.9
MIROC5	74.6	26.9	19.6	−0.7	99.8	5.9	5.6	0.7
CANESM2	33.2	50.7	37.7	0.9	84.5	6.7	5.4	0.6

de Recherches Meteorologiques Coupled Global Climate Model, version 5) and GFDL-ESM2M (Geophysical Fluid Dynamics Laboratory Earth System Model with MOM, version 4 component) AOGCMs have the highest correlation and lowest error for rainfall and temperature variables for baseline 1976–2005, respectively. The CNRM-CM5 and the GFLDL-ESM2M were chosen to project rainfall and temperature in two future periods, respectively.

Calculation of Climate Change Scenarios and Projection of Future Climate Parameters

The CNRM-CM5 and GFDL-ESM2M models were used to simulate rainfall and temperature, respectively, under RCP2.6, RCP4.5, and RCP8.5. The results are listed in Table 4. The effect of climate change was investigated for the two main rivers of the Karkheh basin, namely, Seymareh and Karkheh Rivers.

It is seen in Table 4 the highest temperature of the Seymareh River basin in 2040–2069 would be higher than the maximum temperature of the basin in baseline by 2.5°C, 3.3°C, and 3.8°C under RCP2.6, RCP4.5, and RCP8.5, respectively; in 2070–2099 the increase would equal 2.6°C, 3.5°C, and 6°C under RCP2.6, RCP4.5, and RCP8.5, respectively. In 2040–2069 the range of rainfall change in the Seymareh River basin under RCP2.6 in different seasons would be −75% to 108%; in 2070–2099 and RCP2.6 it would be −100% to 26.5%. The range of rainfall changes in 2040–2069 under RCP4.5 in different seasons would be −42% to 50%; in

Table 4. Results of climate change scenarios [changes in period (2040–2069 or 2070–2099) relative to baseline]

River	Scenario	Change facto	Changes in period compared to baseline	January	February	March	April	May	June	July	August	September	October	November	December
Seymareh	RCP2.6	ΔRAI	2040–2069	2.1	1.2	1	0.7	0.9	0.8	0.2	0.3	1.8	1.1	1.7	0.8
			2070–2099	1.2	1.1	1.2	0.7	0.7	1.2	0	0.4	1.1	1.3	1.2	0.6
		ΔTEM	2040–2069	0.4	1.2	1.5	0.5	1.3	1.2	0.9	1.5	2.5	1.5	0.2	1.3
			2070–2099	0.7	0.7	1.3	0.2	1.2	1	1.2	1.5	2.3	1.7	1.1	1.1
	RCP4.5	ΔRAI	2040–2069	1.5	0.8	1.2	0.7	0.5	0.9	1.5	0.6	1.2	1.4	1	0.6
			2070–2099	2.1	1.2	1.1	0.8	0.8	1.1	1	0.6	1.8	1.1	1.3	0.6
		ΔTEM	2040–2069	1.4	1.1	1.1	1.9	2	2.4	1.6	2.2	3.3	2	1	1.4
			2070–2099	1.3	1.1	2.2	1.4	1.9	2.5	2.4	2.6	3.5	1.8	1.4	1.9
	RCP8.5	ΔRAI	2040–2069	1	1	0.9	0.8	0.6	0.8	0.2	0.3	0.9	0.8	1.2	0.8
			2070–2099	1.7	0.7	0.8	1.1	0.7	0.9	0.2	1	1.1	0.6	1.1	0.7
		ΔTEM	2040–2069	1.6	1.9	2.6	.1	2.8	2.5	2.6	3.2	3.8	2.8	2.3	2.6
			2070–2099	3	3.6	4.1	3.3	4.3	4.5	4.9	5	6	4.7	3.7	4
Karkheh	RCP2.6	ΔRAI	2040–2069	1.4	1.1	0.9	0.9	1	0.8	0.9	0.5	1.5	1.1	1.7	0.9
			2070–2099	1	1	0.9	0.8	0.9	1	0.6	0.6	0.9	1.4	1.3	0.6
		ΔTEM	2040–2069	0.5	1.1	1.3	0.3	1.2	1.2	1	1.4	2.4	1.7	0.2	1.3
			2070–2099	0.8	0.7	1.3	0	1.1	0.9	1.2	1.3	2.4	1.9	1.1	2.3
	RCP4.5	ΔRAI	2040–2069	1.1	0.9	0.9	0.9	0.7	0.7	1.4	0.8	1.3	1.3	1.3	0.8
			2070–2099	1.5	1.1	1	1	0.9	0.7	0.7	1	1.5	1.4	1.4	0.7
		ΔTEM	2040–2069	1.4	1.1	1.1	1.8	2	2.4	1.9	2.3	3.3	2.1	0.9	1.5
			2070–2099	1.5	1	2.1	1.2	1.7	2.5	2.6	2.7	3.5	2	1.4	1.9
	RCP8.5	ΔRAI	2040–2069	1	1.1	0.8	0.9	0.8	0.7	1	0.5	0.8	0.9	1.4	0.9
			2070–2099	1.4	0.7	0.6	1.2	0.6	0.6	0.9	1.3	0.8	0.6	1.2	0.7
		ΔTEM	2040–2069	1.6	1.8	2.5	2	2.8	2.5	2.6	3.3	4	3.1	2.4	2.7
			2070–2099	3.1	3.4	3.9	3.2	4.2	4.4	5.1	5	6.3	5	3.9	4.1

2070–2099 under RCP4.5 it would be −42% to 107%. Under RCP8.5 in 2040–2069 the rate of rainfall change in different seasons would be −75% to 22.2%; in 2070–2099 under RCP8.5 it would be −75% to 73.8%. The range of Karkheh temperature increase in 2040–2069 under RCP2.6, RCP4.5, and RCP8.5 compared to the baseline period's temperature would be 0.2°C–2.4°C, 0.9°C–3.3°C, and 1.6°C–4°C, respectively. The maximum temperature change in Karkheh in 2070–2099 would be under RCP8.5, the maximum temperature change would be 6.3°C higher than baseline periods, and the minimum temperature change is under RCP2.6. The range of Karkheh rainfall changes in 2040–2069 under RCP2.6 in different seasons would be −45% to 67.7%; in 2070–2099 it would be −42% to 45%. Climate projections associated with RCP4.5 in 2040–2069 produce a range of rainfall change in different seasons that would be −32% to 45%; in 2070–2099 under RCP4.5 it would be −30% to 51%. The range of rainfall changes in 2040–2069 under RCP8.5 in different seasons would be −45% to 42%; in 2070–2099 under RCP8.5 it would be −93% to 38%.

Downscaled temperature and rainfall are calculated under climate change scenarios using Eqs. (7) and (8), respectively, and results are presented as the minimum, average, and maximum temperature and rainfall corresponding to RCP2.6, RCP4.5, and RCP8.5 in Table 5. Table 5 shows that the temperature in Seymareh and Karkheh River basin would increase in two future periods under climate change scenarios, and the rate of temperature increase would be highest in future periods under RCP8.5. Long-term monthly changes of Seymareh rainfall in 2040–2069 under RCP2.6, RCP4.5, and RCP8.5 compared to baseline would be an increase equal to 23.2%, a decrease of 3%, and an increase of 0.1%, respectively; changes in rainfall under RCP2.6, RCP4.5, RCP8.5 in 2070–2099 would be a decrease of 0.4%, an increase of 22.8%, and an increase of 6.2%, respectively. Long-term monthly changes of Karkheh rainfall in 2040–2069 compared to the baseline corresponding to RCP2.6, RCP4.5, and RCP8.5 would be an increase of 13.8%, a decrease of 2.2%, and an increase of 3.4%, respectively; change in rainfall in 2070–2099 under RCP2.6, RCP4.5, and RCP8.5 would be

Table 5. Minimum, average, and maximum temperature and rainfall in future

			2040–2069			2070–2099		
River	Scenario	Climate variable	Min	Ave	Max	Min	Ave	Max
Seymareh	RCP2.6	Rainfall (mm)	0	42	331	0	34	228
		Temperature (°C)	0.3	15	28	0.3	15	29
	RCP4.5	Rainfall (mm)	0	33	202	0	40	287
		Temperature (°C)	0.6	16	29	0.6	16	30
	RCP8.5	Rainfall (mm)	0	64	231	0	67	241
		Temperature (°C)	5	17	30	7	18	32
Karkheh	RCP2.6	Rainfall (mm)	0	48	232	0	41	300
		Temperature (°C)	9	25	38	10	25	39
	RCP4.5	Rainfall (mm)	0	41	300	0	47	245
		Temperature (°C)	13	26	39	13	26	40
	RCP8.5	Rainfall (mm)	0	42	255	0	39	224
		Temperature (°C)	11	27	40	12	28	43

a decrease of 3%, an increase of 12%, and an increase of 0.3%, respectively.

The RCP scenarios are classified as pessimistic, optimistic, or intermediate scenarios. Yet, this does not mean that the rainfall forecasts corresponding to the RCP4.5 fall between those of the RCP2.6 and RCP8.5. Zolghadr-Asli (2017), for instance, showed that the global average temperature for RCP8.5 is higher than those corresponding to the RCP2.6 and RCP4.5 scenarios, but this does not mean that precipitation and temperature always follow that pattern of magnitude ordering. Obahoundje et al. (2021), for example, showed that rainfall forecasts based on the models of the IPCC's AR5 associated with the RCPs does not show a definite trend.

Runoff Simulation

This work applied seven neurons based on trial-and-error analysis. Expansion of the training data was implemented to prevent overfitting. The network architecture is of the feed forward neural network type. The activity function is a hyperbolic tangent and the feed network type is a single layer. The learning rule is an algorithm that improves neural network parameters to produce the desired output based on network inputs. This learning process improves weights. This work applied the Levenberg-Marquardt learning technique.

Monthly temperature, rainfall, and river flow were used for ANN training and testing in the Seymareh River using data from climatological station Polechehr, the Ghorbaghistan rain gauge, and the Nazarabad hydrometry station. Concerning the Karkheh River, the 1976–2005 data from the Abdul Khan, Chamgaz, and Gelolgir stations were used. The correlation coefficient and error criteria shown in Table 6 indicate the simulation for period 1986–2005 (for training) and 1976–1985 (for testing) had the best performance with respect to runoff simulation. The results of runoff simulation in two future periods are shown in Table 7, where it is shown that the Seymareh River runoff in two future periods under climate change scenarios would be significantly reduced compared to baseline, and runoff decline in 2070–2099 would be larger than in 2040–2069. The Seymareh River runoff in 2070–2099 would decline by 4%, 4.5%, and 6% under RCP2.6, RCP4.5, and RCP8.5, respectively, compared to baseline. The decline in Seymareh River runoff in 2070–2099 would be largest in May under RCP2.6 and RCP4.5, and decline would be the largest in January under RCP4.5.

Table 6. Results of ANN performance with respect to Seymareh and Karkheh river runoff simulation

River	Parameter	r (%)	NSE	PB (%)	RSR
Seymareh	Train	80	0.6	−0.2	0.6
	Test	75	0.5	7	0.6
Karkheh	Train	77	0.6	0.3	0.3
	Test	78	0.6	6.5	0.3

The Karkheh River runoff in 2040–2069 would decline by 0.7%, 2.1%, and 0.7% under RCP2.6, RCP4.5, and RCP8.5, respectively, compared to baseline; in 2070–2099 it would decline by 0.2%, 0.6%, and 2.6% under RCP2.6, RCP4.5, and RCP8.5, respectively.

The simulation results corresponding to the Seymareh and Karkheh Rivers's runoff show that the average long-term monthly runoff in future periods under climate change scenarios is such that it decreases compared to the baseline period, and this reduction in runoff is due to the reduction in the peak of flood in the two rivers.

Simulation Results for the Operation of Hydropower Reservoirs

The five states of reservoir operation that were investigated are listed in Table 8. Operating states for baseline and future periods were simulated under RCP2.6, RCP4.5, and RCP8.5. Note that the reservoirs studied in this study had not been constructed by 2005, and they were not in operation during baseline. Therefore, simulation of their energy generation in baseline was based on reservoir inflow data applied to the energy generation characteristics of the reservoirs once they were built. Data collected at the Nazarabad and Gelogir hydrometric stations were used in this work (Fig. 3).

The simulation results corresponding to baseline and to the first to fifth states of operation in 2040–2069 and 2070–2099 under RCP2.6, RCP4.5, and RCP8.5 are depicted in Fig. 6. It is evident in Figs. 6(a and b), which depict results corresponding to the first state of operation, that the long-term energy produced by the Sazbon reservoir power plant would increase in the future under RCP2.6, RCP4.5, and RCP8.5 by 2.1%, 2.08%, and 2.05%, respectively, compared to baseline. The smallest percentage change in energy production compared to baseline would be February through May, and the largest change would be in November, when it would increase by 6.4%.

Figs. 6(c and d) show results for the second state of operation, and indicate that the long-term energy production of the Seymareh power plant in 2040–2069 would increase by 5.5%, decrease by 6.3%, and decrease by 9.4% under RCP2.6, RCP4.5, and RCP8.5, respectively, compared to baseline. The largest energy production in 2040–2069 would be 82 GWh in January, and 84 GWh in March and December under RCP2.6; it would be 84 GWh under RCP4.5 in January; and it would be 83 GWh in January and March, and 82 GWh in April and May under RCP8.5.

Figs. 6(e and f) for the third state of operation indicate the long-term energy production of the Seymareh power plant (taking into account the effect of the upstream reservoir, Sazbon) in 2040–2069 would increase by 4%, decrease by 7%, and decrease by 11% under RCP2.6, RCP4.5, and RCP8.5, respectively, compared to baseline. The largest energy production in 2040–2069 would be under RCP2.6, and would be greatest in January, March, May, and December, and the smallest energy production corresponds to

Table 7. Seymareh and Karkheh simulated river runoff under climate change and baseline (m^3/s)

	1976–2005			2040–2069				2070–2099			
River	Min	Ave	Max	Scenario	Min	Ave	Max	Scenario	Min	Ave	Max
Seymareh	6	92	300	RCP2.6	8	95	297	RCP2.6	9	88	226
				RCP4.5	6	85	373	RCP4.5	7	87	385
				RCP8.5	10	82	285	RCP8.5	15	86	261
Karkheh	11	139	422	RCP2.6	10	138	213	RCP2.6	8	139	229
				RCP4.5	9	136	265	RCP4.5	8	138	241
				RCP8.5	9	138	288	RCP8.5	9	135	241

Table 8. States of operation of hydropower reservoirs

Periods	States				
	First	Second	Third	Fourth	Fifth
1976–2005	Sazbon	Seymareh	Sazbon and Seymareh	Seymareh and Karkheh	Sazbon, Seymareh, and Karkheh
2040–2069	Sazbon	Seymareh	Sazbon and Seymareh	Seymareh and Karkheh	Sazbon, Seymareh, and Karkheh
2070–2099	Sazbon	Seymareh	Sazbon and Seymareh	Seymareh and Karkheh	Sazbon, Seymareh, and Karkheh

RCP8.5, which would be the least in August and September (31 GWh).

Figs. 6(g and h) depict results for the fourth state of operation and indicate the energy produced by the Karkheh power plant (taking into account the effect of the upstream reservoir Seymareh) in 2040–2069 would increase by 8.5%, 3%, and 6.8% under RCP2.6, RCP4.5, and RCP8.5, respectively, compared to baseline. The increase in long-term energy produced in 2040–2069 under RCP2.6 and RCP4.5 would be largest in September and October, respectively, and would be 19 and 23 GWh larger than the corresponding month's long-term produced energy in baseline, respectively.

Figs. 6(i and j) display the results corresponding to the fifth state of operation and indicate that the energy produced by the Karkheh power plant (taking into account the effect of upstream reservoirs Sazbon and Seymareh) in 2040–2069 would increase by 7.8%, 1.9%, and 6.5% under RCP2.6, RCP4.5, and RCP8.5, respectively, compared to baseline.

The energy produced depends on the reservoir inflow, and especially on its pattern. For example, the Seymareh River runoff declines under climate change compared to the baseline, but the pattern of the runoff is such that it declines under climate change from September through November, and it rises from February through May (peaking in April). Also, the effect of runoff reduction in the future periods compared to the baseline, for example at Sazbon power plant, is reducing the reservoir spill, which has no effect on energy production. The reduction in energy production is caused by a decrease in future runoff (from September through November).

Conversely, the Sazbon and Seymareh power plants, which have a series connection and are a short distance from each other, generate energy in a distinct manner. Specifically, it is seen in Fig. 7 that the effect of declining runoff in future periods compared to the baseline is a reduction in the energy production at the Sazbon power plant. The reduction in peak runoff is ineffective in energy production. This is so because only the reservoir spill would be reduced in future periods compared to the baseline. According to Fig. 8, the effect of reducing the flood peak in future periods compared to the baseline period on energy production at the Seymareh power plant is significant, so that in the baseline period the maximum hydropower energy is produced in the months when the flood peak occurs, and the reduction of flood peak in the future periods would drastically reduce energy production. The energy produced in the two-reservoir and three-reservoir systems is governed by the water releases from the upstream reservoir, and by the volume of interbasin runoff. For example, for the two-reservoir system comprising Karkheh with Seymareh reservoirs located upstream, the capacity of the Seymareh power plant is larger than that of Karkheh power plant, and therefore the reservoir releases are such that downstream demands of the Seymareh power plant are not met, but the production capacity of Karkheh power plant is met.

The inflow to the reservoir and the reservoir water releases in baseline and two future periods corresponding to the first to fifth states of operation are listed in Table 9. The results in Table 9 indicate the annual inflow to Sazbon reservoir and the annual reservoir release corresponding to the first state of operation under climate change would decline significantly. Annual inflow in 2040–2069 under climate change scenarios would increase 4%, decrease 6.6%, and decrease 10.4%, respectively, compared to baseline, and it would decrease 4%, 4.6%, and 6.2%, respectively, in the 2070–2099 compared to baseline. Annual release in 2040–2069 under climate change scenarios would increase 3.9%, decrease 6.7%, and decrease 10.4%, respectively, compared to baseline, and in 2070–2099 it would decrease 4.1%, 4.9%, and 6.4%, respectively, compared to baseline. The annual inflow to Seymareh reservoir and the annual reservoir release corresponding to the second state of operation under climate change would decline significantly, and the reductions would be largest in 2040–2069 under RCP8.5. The percentage of annual inflow changes to the Seymareh single-reservoir system in 2040–2069 would increase by 4%, decrease by 6.5%, and decrease by 10.4% under RCP2.6, RCP4.5, and RCP8.5, respectively, compared to baseline. The percentage of annual changes in reservoir release in 2070–2099 would decrease by 3.8%, 4.4%, and 6.1%, under RCP2.6, RCP4.5, and RCP8.5, respectively, compared to baseline. The annual inflow and reservoir releases would be significantly reduced in the third state of operation during the two periods of climate change considered in this paper compared to baseline. The reduction of annual inflow and reservoir release in 2040–2069 would be 6.7% under RCP4.5 compared to baseline. Annual inflow in 2070–2099 would decline by 4.1%, 4.8%, and 6.4% under RCP2.6, RCP4.5, and RCP8.5, respectively, compared to baseline; the annual reservoir release would decline by 3.9%, 4.7%, and 6.3% under RCP2.6, RCP4.5, and RCP8.5, respectively, compared to baseline. Results for the fourth state of operation indicate the annual inflow in 2040–2069 would decline by 6.9%, 13%, and 7.8% under RCP2.6, RCP4.5, and RCP8.5, respectively, compared to baseline; in 2070–2099 the annual inflow would decline by 15.6%, 10.3%, and 10.7% under RCP2.6, RCP4.5, and RCP8.5, respectively, compared to baseline. Results corresponding to the fifth state of operation indicate that changes of annual reservoir inflow and annual release are the same in periods of climate change, so that in 2040–2069 it would decrease by 7.2%, 13.3%, and 7.8% under RCP2.6, RCP4.5, and RCP8.5, respectively, relative to baseline; in 2070–2099 annual inflow would decline by 15.9%, 11%, and 10.6% under RCP2.6, RCP4.5, and RCP8.5, respectively, compared to baseline.

Efficiency Indexes of Reservoir Energy Generation

Efficiency indexes corresponding to the first through fifth states of operation in baseline and future periods were calculated under RCP2.6, RCP4.5, and RCP8.5. The results are listed in Table 10, where it is seen the efficiency indexes for example in the first state of operation in periods of climate change are improved compared to baseline. In this state of operation, the inflow to the reservoir decreases during periods of climate change, the storage volume of the reservoir increases, and the release decreases relative to baseline. In fact, it can be said that the reduction of runoff reduces the nonpeak energy. Also, the second state of operation's time reliability in 2040–2069 would decline by 2%, 26%, and 18% under RCP2.6, RCP4.5, and RCP8.5, respectively, compared to baseline; in 2070–2099 the time reliability would decline by 18%, 28%, and 32%

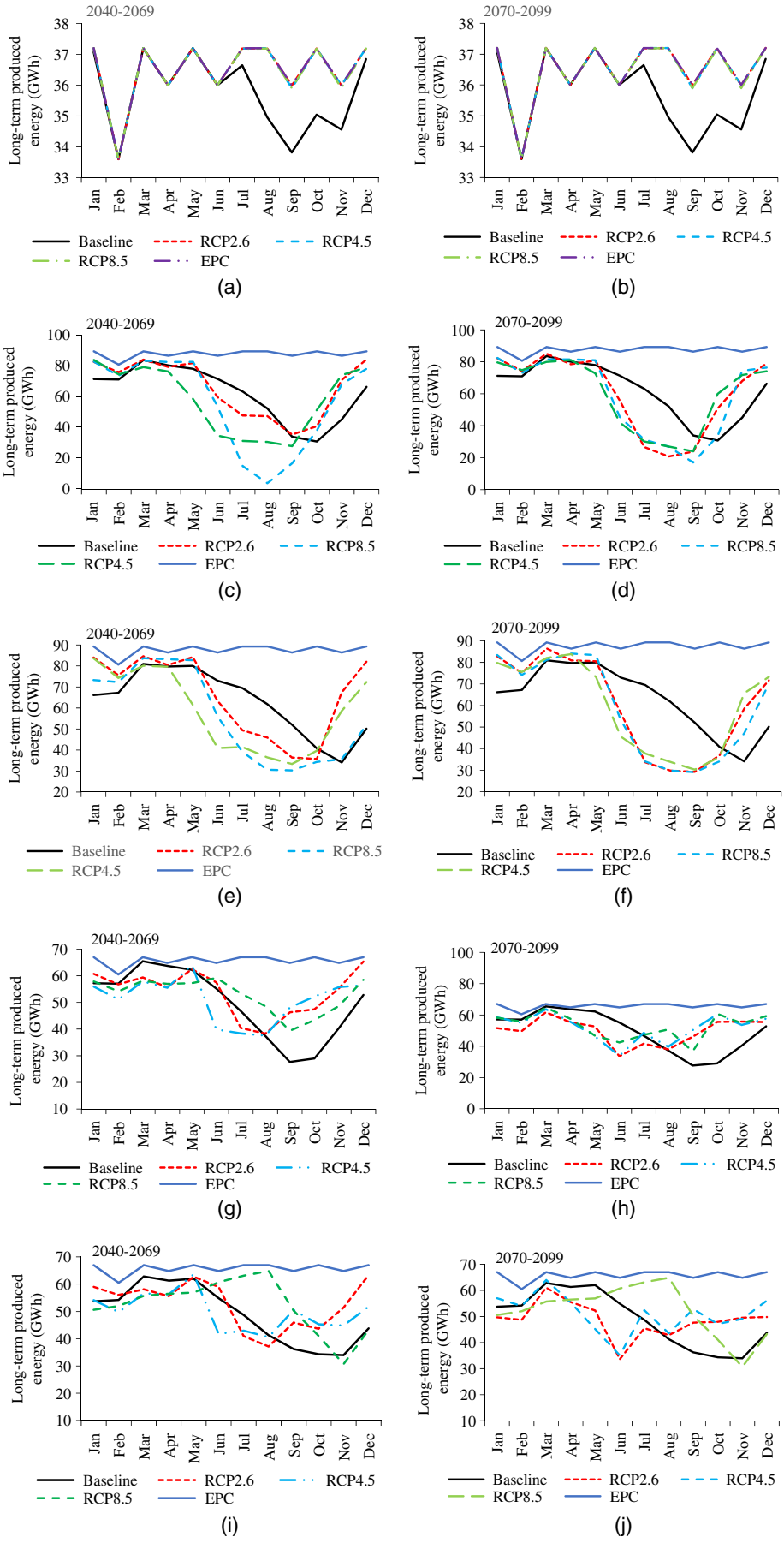

Fig. 6. Comparison of long-term energy production in the baseline and future periods corresponding to the first through fifth states of operation under RCP2.6, RCP4.5, and RCP8.5 with energy production capacity in (a, c, e, g, and i) 2040–2069; and (b, d, f, h, and j) 2070–2099.

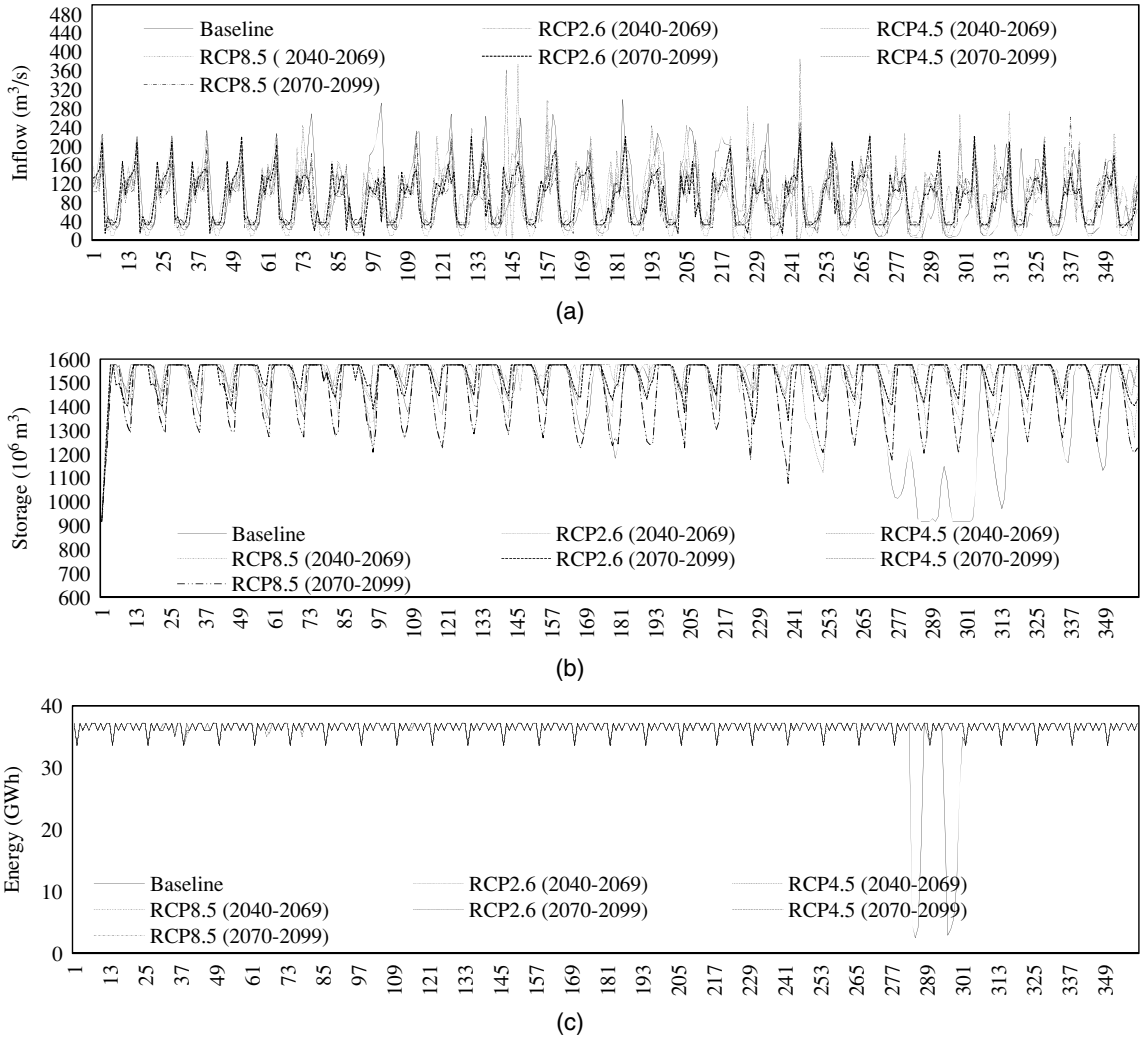

Fig. 7. (a) Reservoir inflow; (b) reservoir storage volume; and (c) energy produced by Sazbon power plant.

under RCP2.6, RCP4.5, and RCP8.5, respectively. Volumetric reliability in 2040–2069 would increase by 5.5%, decrease by 5.5%, and decrease by 9.6% under RCP2.6, RCP4.5, and RCP8.5, respectively, compared to baseline; in 2070–2099 volumetric reliability would decline by 2.7%, 4.1%, and 5.5% under RCP2.6, RCP4.5, and RCP8.5, respectively, compared to baseline. The largest percentage of volumetric reliability change in 2040–2069 and 2070–2099 corresponds to RCP8.5, which would be highest in 2040–2069. Vulnerability would rise significantly, and in 2070–2099 it would rise by 12%, 12%, and 20% under RCP2.6, RCP4.5, and RCP8.5, respectively, compared to baseline. Vulnerability in 2040–2069 would be highest under RCP8.5 (with a 76% increase compared to baseline). Resiliency in 2040–2069 would increase by 24%, 6%, and 12% under RCP2.6, RCP4.5, and RCP8.5, respectively, compared to baseline; resiliency would increase in 2070–2099 by 5.8% under RCP2.6 and RCP8.5 and it is unchanged for RCP4.5, compared to baseline. The resiliency of the system would be higher in 2040–2069 under RCP2.6 (11.7%). Sustainability in future periods under climate change scenarios would decline relative to baseline. Availability in 2040–2069 would decrease compared to baseline by 2%, 26%, and 18% under RCP2.6, RCP4.5, and RCP8.5, respectively; in 2070–2099 it would decrease by 18%, 28%, and 32% under RCP2.6, RCP4.5, and RCP8.5, respectively, compared to baseline. The decline in the availability index in 2070–2099 would be larger than in 2040–2069. Supply-to-demand in 2040–2069 would decrease by 7.8%, 11.7%, and 4% under RCP2.6, RCP4.5, and RCP8.5, respectively, compared to baseline; in 2070–2099 supply-to-demand would decline by 9%, 15.6%, and 17% under RCP2.6, RCP4.5, and RCP8.5, respectively, compared to baseline. Also, results corresponding to the other states of operation (third, fourth, and fifth) indicate the efficiency indexes of reservoir energy generation will change under RCPs in future periods compared baseline.

Conclusion

This study evaluated the effect of climate change on hydropower energy production corresponding to five operating states in 2040–2069 and 2070–2099. Energy generation was evaluated with seven efficiency indexes based on a system dynamics approach. Evaluation of climate projections by 17 AOGCMs presented in IPCC's Fifth Assessment Report revealed that CNRM-CM5 and GFDL-ESM2M models had the best correlation and the lowest error for rainfall and temperature, respectively. ANN results for the Seymareh and Karkheh Rivers under RCP2.6, RCP4.5, and RCP8.5 in 2040–2069 and 2070–2099 indicate that Seymareh River runoff in two future periods would decline in comparison with baseline. Karkheh runoff would decline in two future periods

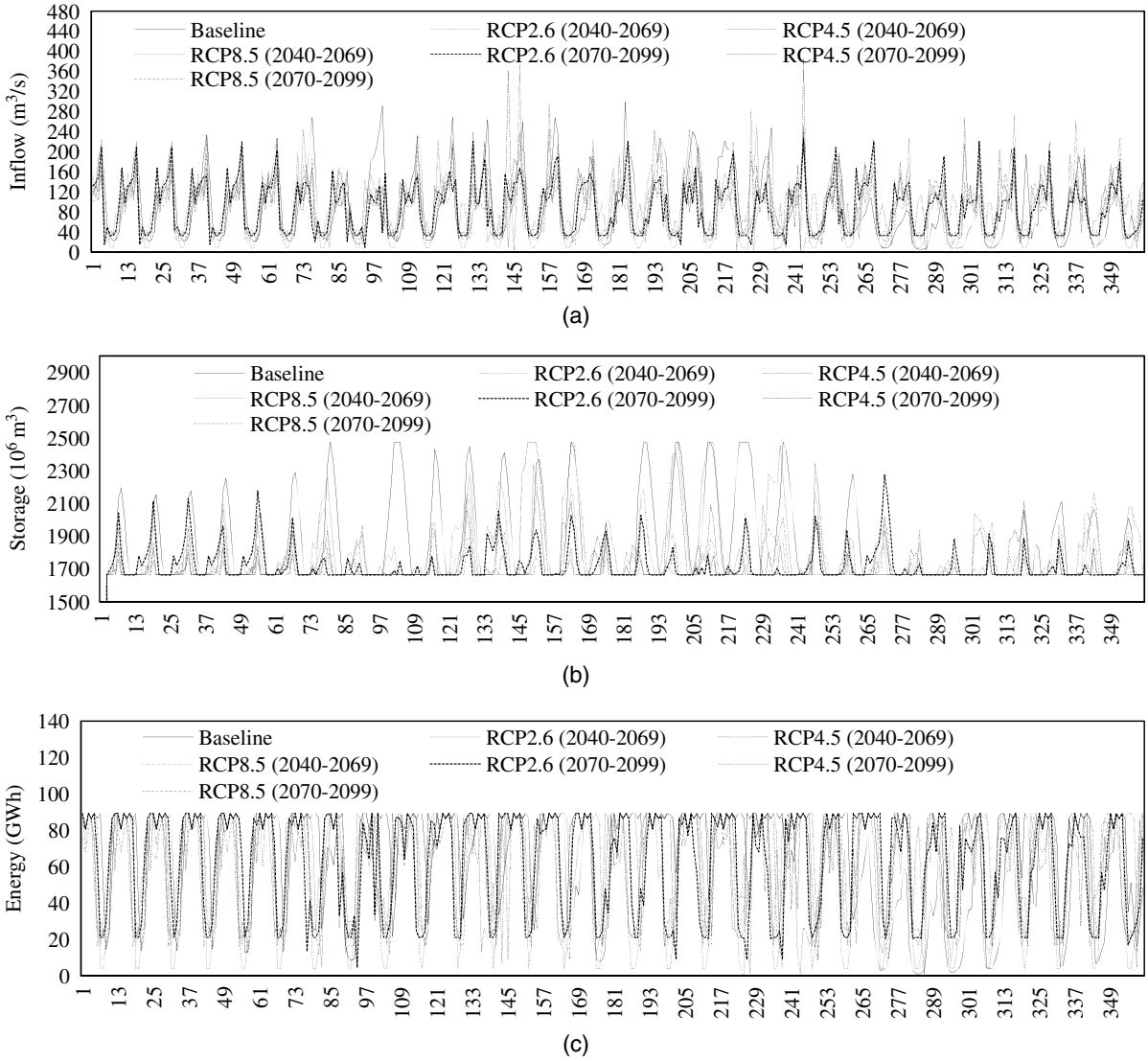

Fig. 8. (a) Reservoir inflow; (b) reservoir storage volume; and (c) energy produced by Seymareh power plant.

Table 9. Annual reservoir inflow and release for the states of operation (Seymareh reservoir) in baseline and climate change

		2040–2069			2070–2099		
Characteristics	Baseline	RCP2.6	RCP4.5	RCP8.5	RCP2.6	RCP4.5	RCP8.5
			First state				
Annual inflow ($\times 10^6$ m^3)	2,869	2,984	2,680	2,569	2,754	2,738	2,691
Annual release ($\times 10^6$ m^3)	2,787	2,897	2,598	2,496	2,672	2,651	2,608
			Second state				
Annual inflow ($\times 10^6$ m^3)	2,869	2,984	2,681	2,569	2,754	2,737	2,691
Annual release ($\times 10^6$ m^3)	2,779	2,901	2,599	2,488	2,672	2,656	2,610
			Third state				
Annual inflow ($\times 10^6$ m^3)	2,787	2,897	2,598	2,496	2,671	2,651	2,608
Annual release ($\times 10^6$ m^3)	2,698	2,815	2,517	2,416	2,591	2,570	2,528
			Fourth state				
Annual inflow ($\times 10^6$ m^3)	4,461	4,152	3,881	4,111	3,762	3,982	3,999
Annual release ($\times 10^6$ m^3)	4,449	4,141	3,870	4,100	3,752	3,971	3,989
			Fifth state				
Annual inflow ($\times 10^6$ m^3)	4,380	4,066	3,799	4,039	3,681	3,896	3,917
Annual release ($\times 10^6$ m^3)	4,368	4,055	3,789	4,028	3,671	3,885	3,907

under the three scenarios of climate change compared to baseline. This work's results show the long-term energy production associated with the first state of operation in future periods under RCP2.6, RCP4.5, and RCP8.5 would increase by 2.1%. Results corresponding to second state of reservoir operation indicate the long-term energy production in 2040–2069 would increase by 5.5%, decrease by 6.3%, and decrease by 9.4% under RCP2.6, RCP4.5, and RCP8.5, respectively, compared to baseline; in 2070–2099 long-term energy production would decrease by 2.8%, 3.9%, and 5.6% under RCP2.6, RCP4.5, and RCP8.5, respectively, compared to baseline. Results corresponding to the third operation state indicate the long-term energy production in 2040–2069 would rise by 4%, decrease by 7%, and decrease by 11% under RCP2.6, RCP4.5, and RCP8.5, respectively, compared to baseline; in 2070–2099 long-term energy production would decline by 4%, 5%, and 7% under RCP2.6, RCP4.5, and RCP8.5 scenarios, respectively, compared to baseline. Results corresponding to fourth operation state indicate long-term energy production in 2040–2069 would rise by 8.5%, 3%, and 6.8% under RCP2.6, RCP4.5, and RCP8.5, respectively, compared to baseline; in 2070–2099 the long-term energy production would decline by 0.4%, and it would rise by 4.8% and 6.7% under RCP2.6, RCP4.5, and RCP8.5,

Table 10. Efficiency indexes for the second to fifth states of operation (%)

States	Index	Production capacity (%)	Baseline	2040–2069			2070–2099		
				RCP2.6	RCP4.5	RCP8.5	RCP2.6	RCP4.5	RCP8.5
First	Time reliability	100	97	99	99	98	99	99	99
	Volume reliability		98	99	99	99	99	99	98
	Vulnerability		2	0.002	0.002	0.001	0.003	0.001	0.002
	Resiliency		25	50	99	98	98	98	98
	Sustainability		23	50	99	99	99	99	98
	Availability		97	99	98	98	99	99	99
	Supply to demand		98	99	98	99	98	98	98
Second	Time reliability	100	50	49	37	41	41	36	34
		90	70	70	58	56	56	54	52
		75	83	98	83	76	86	86	88
	Volume reliability	100	73	77	69	66	71	70	69
		90	86	86	76	74	71	78	77
		75	89	99	91	89	75	94	94
	Vulnerability	100	25	22	30	44	28	28	30
		90	12	12	22	32	19	21	21
		75	10	1	8	24	4	5	5
	Resiliency	100	17	21	18	19	18	17	18
		90	30	30	24	32	21	28	21
		75	43	57	36	33	40	50	44
	Sustainability	100	6	8	4	5	6	4	4
		90	18	18	10	9	9	12	8
		75	25	55	28	21	33	38	36
	Availability	100	50	49	37	41	41	36	34
		90	69	69	58	56	56	54	52
		75	83	98	83	76	86	86	88
	Supply to demand	100	77	71	68	74	70	65	64
		90	82	82	81	81	76	75	75
		75	93	98	91	86	91	91	93
Third	Time reliability	100	47	43	30	28	35	34	30
		90	57	65	50	42	51	51	47
		75	80	96	77	74	84	81	81
	Volume reliability	100	71	75	66	64	68	68	67
		90	79	84	74	72	77	76	75
		75	89	98	89	87	93	92	92
	Vulnerability	100	27	25	32	35	30	31	32
		90	20	14	24	27	21	22	23
		75	10	1	1	12	6	7	7
	Resiliency	100	13	17	14	14	16	14	15
		90	16	28	16	15	17	28	18
		75	10	50	31	26	34	40	38
	Sustainability	100	4	5	2	2	4	3	3
		90	7	15	5	4	7	11	6
		75	7	47	21	17	27	30	30
	Availability	100	47	43	30	28	35	34	31
		90	57	65	46	42	51	51	47
		75	80	96	78	74	84	81	81
	Supply to demand	100	75	68	63	64	66	65	63
		90	78	80	71	70	73	74	71
		75	91	98	88	86	91	89	89

Table 10. (*Continued*.)

States	Index	Production capacity (%)	Baseline	2040–2069			2070–2099		
				RCP2.6	RCP4.5	RCP8.5	RCP2.6	RCP4.5	RCP8.5
Fourth	Time reliability	100	39	27	17	21	16	19	17
		90	45	44	34	35	29	39	42
		75	56	68	61	61	43	61	64
	Volume reliability	100	75	80	77	80	75	79	80
		90	81	88	83	86	82	86	87
		75	88	95	92	93	89	92	93
	Vulnerability	100	24	17	22	20	23	20	20
		90	18	11	15	13	17	13	12
		75	11	4	6	6	10	7	6
	Resiliency	100	13	21	14	16	14	16	16
		90	15	35	22	24	26	30	35
		75	26	65	48	46	41	54	54
	Sustainability	100	4	4	2	2	2	2	2
		90	5	13	6	7	6	10	13
		75	13	43	27	27	18	30	32
	Availability	100	39	27	18	21	17	19	18
		90	45	44	34	35	29	39	42
		75	56	68	61	61	48	61	64
	Supply to demand	100	86	45	40	41	41	40	37
		90	64	56	50	48	47	53	54
		75	67	72	69	68	58	68	71
Fifth	Time reliability	100	38	25	16	24	15	18	17
		90	44	44	30	44	27	33	36
		75	54	64	60	57	46	58	62
	Volume reliability	100	74	80	75	79	74	77	78
		90	79	85	82	84	80	84	85
		75	87	95	91	90	88	92	92
	Vulnerability	100	25	19	23	20	25	22	20
		90	19	13	17	14	19	15	14
		75	12	4	8	9	10	7	7
	Resiliency	100	12	20	13	12	13	15	16
		90	15	34	21	29	22	25	32
		75	23	61	41	41	41	50	51
	Sustainability	100	3	4	1	2	1	2	3
		90	5	13	5	11	5	7	10
		75	11	37	22	21	16	27	30
	Availability	100	38	26	16	24	15	18	17
		90	44	44	30	44	27	33	36
		75	54	64	60	57	46	59	62
	Supply to demand	100	63	45	40	45	41	41	38
		90	64	57	48	59	46	49	50
		75	67	70	68	67	57	67	69

respectively, compared to baseline. The percentage change in long-term energy production associated with fifth operation state in 2040–2069 would increase by 8%, 2%, and 6.5% under RCP2.6, RCP4.5, and RCP8.5, respectively, relative to baseline; in 2070–2099 long-term energy production would decline by 0.5%, and increase by 4.2% and 6.5% under RCP2.6, RCP4.5, and RCP8.5, respectively, compared to baseline. Seven efficiency indexes of hydropower production were calculated and their values vary across the five operation states. For example, time reliability declines relative to baseline in third state of operation over two future periods. The decline in time reliability in 2070–2099 is less than 2040–2069. The volumetric reliability declines in two future periods compared to baseline, and decline is more severe in 2040–2069 under RCP8.5. Vulnerability would rise in two future periods compared to baseline, and the system would be most vulnerable in 2040–2069 under RCP8.5. The efficiency indexes corresponding to energy production targets equal to 90% and 75% of production capacity are better in baseline and two future periods than those associated with an energy production target equal to 100% of installed capacity.

This paper's approach for evaluating policies for operation of hydropower reservoirs under climate change conditions using various efficiency indexes provides valuable guidance to assist in management of future hydropower energy generation. Hydropower plants are sensitive and vulnerable to climate change and the impact of climate change on hydropower across regions is heterogeneous (Fan et al. 2020). This research and previous studies (Qin et al. 2020) show that hydropower generation under climate change exhibits a nonlinear pattern. These findings highlight the complexity of managing and generating hydropower plants under climate change scenarios (Sarzaeim et al. 2018).

Improving optimal performance of hydropower plants is possible if decision makers take into account multiple criteria, in particular, reliability, flexibility, and vulnerability (Mateus and Tullos 2017). This work measures the performance of multireservoir hydropower system in baseline and under climate change conditions based on the

indexes of vulnerability, resiliency, reliability, flexibility, availability, and supply-to-demand. Vulnerability calculates the system damage over the operation period. Vulnerability measures what percentage of the energy capacity is not delivered (downstream demands). For example, the vulnerability of the Seymareh single-reservoir system would increase by 12%, 12%, and 20% in the future period compared to the baseline under RCP2.6, RCP4.5, and RCP8.5 scenarios, respectively. This means that the system under the RCP2.6 scenario would not meet 12% of the downstream demands. The vulnerability may be low, but system damage may occur. For example, the period required to return to normal operation requires a longer time, and this means that the system has suffered damage. The volumetric reliability index determines the total deficit during the operation period, while the time reliability calculates the sum of the total monthly failures of the system (periods when the system does not supply the power plant's energy generation capacity). The higher the time reliability, the better the performance of the system, but other phenomena, such as population growth, may increase downstream demand, and in some cases even a change in the dam's function under climate change. The flexibility index expresses the capacity of the system to withstand the negative effects of climate change. For example, flexibility decreases in future periods under climate change scenarios compared to the baseline in the Seymareh single-reservoir system. This means that the system would not cope well with deficits under climate change while sustaining minimal damage.

Data Availability Statement

The data that support the findings of this study are available from the corresponding author upon reasonable request.

References

Adynkiewicz-Piragas, M., and B. Miszuk. 2020. "Risk analysis related to impact of climate change on water resources and hydropower production in the Lusatian Neisse river basin." *Sustainability* 12 (12): 5060. https://doi.org/10.3390/su12125060.

Alimohammadi, H., A. R. Massah Bavani, and A. Roozbahani. 2020. "Mitigating the impacts of climate change on the performance of multi-purpose reservoirs by changing the operation policy from SOP to MLDR." *Water Resour. Manage.* 34 (4): 1495–1516. https://doi.org/10.1007/s11269-020-02516-5.

ASCE. 1998. *Sustainability criteria for water resources systems*. Task Committee on Sustainability Criteria, Water Resources Planning and Management Division, ASCE and Working Group, UNESCO/IHP IV Project M-4.3. Reston, VA: ASCE.

Ashofteh, P.-S., T. Rajaee, P. Golfam, and X. Chu. 2019. "Applying climate adaptation strategies for improvement of management indexes of a river–reservoir irrigation system." *Irrig. Drain.* 68 (3): 420–432. https://doi.org/10.1002/ird.2336.

Boadi, S. A., and K. Owusu. 2019. "Impact of climate change and variability on hydropower in Ghana." *Afr. Geog. Rev.* 38 (1): 19–31. https://doi.org/10.1080/19376812.2017.1284598.

Chen, J., H. Y. Shi, B. Sivakumar, and M. R. Peart. 2016. "Population, water, food, energy and dams." *Renewable Sustainable Energy Rev.* 56 (Apr): 18–28. https://doi.org/10.1016/j.rser.2015.11.043.

Chilkoti, V., T. Bolisetti, and R. Balachandar. 2017. "Climate change impact assessment on hydropower generation using multi-model climate ensemble." *Renewable Energy* 109 (Aug): 510–517. https://doi.org/10.1016/j.renene.2017.02.041.

Dallison, R. J. H., S. D. Patil, and A. P. Williams. 2021. "Impacts of climate change on future water availability for hydropower and public water supply in Wales, UK." *J. Hydrol.: Reg. Stud.* 36 (Aug): 100866. https://doi.org/10.1016/j.ejrh.2021.100866.

Fan, J.-L., J.-W. Hu, X. Zhang, L.-S. Kong, F. Li, and Z. Mi. 2020. "Impacts of climate change on hydropower generation in China." *Math. Comput. Simul.* 167 (Jan): 4–18. https://doi.org/10.1016/j.matcom.2018.01.002.

Gupta, H. V., S. Sorooshian, and P. O. Yapo. 1999. "Status of automatic calibration for hydrologic models: Comparison with multilevel expert calibration." *J. Hydrol. Eng.* 4 (2): 135–143. https://doi.org/10.1061/(ASCE)1084-0699(1999)4:2(135).

Hashimoto, T., J. R. Stedinger, and D. P. Loucks. 1982. "Reliability, resiliency and vulnerability criteria for water resources system performance evaluation." *Water Resour. Res.* 18 (1): 14–20. https://doi.org/10.1029/WR018i001p00014.

IPCC (Intergovernmental Panel on Climate Change). 2013. "Climate change 2013: The physical science basis." In *Contribution of working group I to the fifth assessment rep. of the intergovernmental panel on climate change*, edited by T. F. Stocker. Cambridge, UK: Cambridge University Press.

Jamali, S., A. Abrishamchi, and K. Madani. 2013. "Climate change and hydropower planning in the Middle East: Implications for Iran's Karkheh hydropower systems." *J. Energy Eng.* 139 (3): 153–160. https://doi.org/10.1061/(ASCE)EY.1943-7897.0000115.

Jones, P. D., and M. Hulme. 1996. "Calculating regional climate times series for temperature precipitation: Methods and illustrations." *Int. J. Climatol.* 16 (4): 361–377. https://doi.org/10.1002/(SICI)1097-0088(199604)16:4<361::AID-JOC53>3.0.CO;2-F.

Kim, W., J. Lee, J. Kim, and S. Kim. 2019. "Assessment of water supply stability for drought-vulnerable Boryeong multipurpose dam in South Korea using future dry climate change scenarios." *Water* 11 (11): 2403. https://doi.org/10.3390/w11112403.

Li, J., Z. Wang, X. Wu, B. Ming, L. Chen, and X. Chen. 2020. "Evident response of future hydropower generation to climate change." *J. Hydrol.* 590 (Nov): 125385. https://doi.org/10.1016/j.jhydrol.2020.125385.

Liu, B., J. R. Lund, L. Liu, S. Liao, G. Li, and C. Cheng. 2020. "Climate change impacts on hydropower in Yunnan, China." *Water* 12 (1): 197. https://doi.org/10.3390/w12010197.

Loucks, D. P. 1997. "Quantifying trends in system sustainability." *Hydrol. Sci. J.* 42 (4): 513–530. https://doi.org/10.1080/02626669709492051.

Majumder, P., M. Majumder, A. K. Saha, and S. Nath. 2020. "Selection of features for analysis of reliability of performance in hydropower plants: A multi-criteria decision making approach." *Environ. Dev. Sustainability* 22 (4): 3239–3265. https://doi.org/10.1007/s10668-019-00343-2.

Mateus, M. C., and D. Tullos. 2017. "Reliability, sensitivity, and vulnerability of reservoir operations under climate change." *J. Water Resour. Plann. Manage.* 143 (4): 04016085. https://doi.org/10.1061/(ASCE)WR.1943-5452.0000742.

Moriasi, D. N., J. G. Arnold, M. W. Van Liew, R. L. Bingner, R. D. Harmel, and T. L. Veith. 2007. "Model evaluation guidelines for systematic quantification of accuracy in watershed simulations." *Trans. ASABE* 50 (3): 885–900. https://doi.org/10.13031/2013.23153.

Mutsindikwa, T. C., Y. Yira, A. Y. Bossa, J. Hounkpè, S. Salack, I. A. Saley, and A. Rabani. 2021. "Modeling climate change impact on the hydropower potential of the Bamboi catchment." *Model. Earth Syst. Environ.* 7 (4): 2709–2717. https://doi.org/10.1007/s40808-020-01052-w.

Nash, J. E., and J. V. Sutcliffe. 1970. "River flow forecasting through conceptual models, Part I—A discussion of principles." *J. Hydrol.* 10 (3): 282–290. https://doi.org/10.1016/0022-1694(70)90255-6.

Nautiyal, H., and V. Goel. 2020. "Sustainability assessment of hydropower projects." *J. Cleaner Prod.* 265 (Aug): 121661. https://doi.org/10.1016/j.jclepro.2020.121661.

Nguyen, H., R. Mehrotra, and A. Sharma. 2020. "Assessment of climate change impacts on reservoir storage reliability, resilience, and vulnerability using a multivariate frequency bias correction approach." *Water Resour. Res.* 56 (2): e2019WR026022. https://doi.org/10.1029/2019WR026022.

Obahoundje, S., M. Youan Ta, A. Diedhiou, E. Amoussou, and K. Kouadio. 2021. "Sensitivity of hydropower generation to changes in climate and land use in the Mono basin (West Africa) using CORDEX dataset and WEAP model." *Environ. Processes* 8 (3): 1073–1097. https://doi.org/10.1007/s40710-021-00516-0.

Qin, P., H. Xu, M. Liu, L. Du, C. Xiao, L. Liu, and B. Tarroja. 2020. "Climate change impacts on three Gorges reservoir impoundment and hydropower generation." *J. Hydrol.* 580 (Jan): 123922. https://doi.org/10.1016/j.jhydrol.2019.123922.

Ren, K., S. Huang, Q. Huang, H. Wang, G. Leng, W. Fang, and P. Li. 2020. "Assessing the reliability, resilience and vulnerability of water supply system under multiple uncertain sources." *J. Cleaner Prod.* 252 (Apr): 119806. https://doi.org/10.1016/j.jclepro.2019.119806.

Sarzaeim, P., O. Bozorg-Haddad, B. Zolghadr-Asli, E. Fallah-Mehdipour, and H. A. Loáiciga. 2018. "Optimization of run-of-river hydropower plant design under climate change conditions." *Water Resour. Manage.* 32 (12): 3919–3934. https://doi.org/10.1007/s11269-018-2027-0.

Shrestha, A., S. Shrestha, T. Tingsanchali, A. Budhathoki, and S. Ninsawat. 2021. "Adapting hydropower production to climate change: A case study of Kulekhani hydropower project in Nepal." *J. Cleaner Prod.* 279 (Jan): 123483. https://doi.org/10.1016/j.jclepro.2020.123483.

Wang, H., W. Xiao, Y. Wang, Y. Zhao, F. Lu, M. Yang, B. Hou, and H. Yang. 2019. "Assessment of the impact of climate change on hydropower potential in the Nanliujiang river basin of China." *Energy* 167 (Jan): 950–959. https://doi.org/10.1016/j.energy.2018.10.159.

Zeng, P., F. Sun, Y. Liu, and Y. Che. 2020. "Future river basin health assessment through reliability-resilience-vulnerability: Thresholds of multiple dryness conditions." *Sci. Total Environ.* 741 (Nov): 140395. https://doi.org/10.1016/j.scitotenv.2020.140395.

Zhong, W., J. Guo, L. Chen, J. Zhou, J. Zhang, and D. Wang. 2020. "Future hydropower generation prediction of large-scale reservoirs in the upper Yangtze river basin under climate change." *J. Hydrol.* 588 (Sep): 125013. https://doi.org/10.1016/j.jhydrol.2020.125013.

Zhou, Y., S. Guo, C.-Y. Xu, F.-J. Chang, H. Chen, P. Liu, and B. Ming. 2020. "Stimulate hydropower output of mega cascade reservoirs using an improved kidney algorithm." *J. Cleaner Prod.* 244 (Jan): 118613. https://doi.org/10.1016/j.jclepro.2019.118613.

Zolghadr-Asli, B. 2017. "Discussion of 'Multiscale assessment of the impacts of climate change on water resources in Tanzania' by Umesh Adhikari, A. Pouyan Nejadhashemi, Matthew R. Herman, and Joseph P. Messina." *J. Hydrol. Eng.* 22 (8): 07017010. https://doi.org/10.1061/(ASCE)HE.1943-5584.0001553.

Zolghadr-Asli, B., O. Bozorg-Haddad, and X. Chu. 2019. "Effects of the uncertainties of climate change on the performance of hydropower systems." *J. Water Clim. Change* 10 (3): 591–609. https://doi.org/10.2166/wcc.2018.120.